J Mater Sci (2007) 42:346–351
DOI 10.1007/s10853-006-1032-5

Preparation and characterization of Mn-doped $BaTiO_3$ thin films by magnetron sputtering

J. P. Chu · T. Mahalingam · C. F. Liu · S. F. Wang

Received: 12 August 2004 / Accepted: 24 October 2005 / Published online: 20 October 2006

Abstract Barium titanate ($BaTiO_3$) thin films doped with Mn (0.1–1.0 at%) were prepared by r.f. magnetron sputtering technique. Oxygen/argon (O_2/Ar) gas ratio is found to influence the sputtering rate of the films. The effects of Mn doping on the structural, microstructural and electrical properties of $BaTiO_3$ thin films are studied. Mn-doped thin films annealed at high temperatures (700 °C) exhibited cubic perovskite structure. Mn doping is found to reduce the crystallization temperature and inhibit the grain growth in barium titanate thin films. The dielectric constant increases with Mn content and the dielectric loss (tan δ) reveals a minimum value of 0.0054 for 0.5% Mn-doped $BaTiO_3$ films measured at 1 MHz. The leakage current density decreases with Mn doping and is 10^{-11} A/cm^{-2} at 6 kV/cm for 1% Mn-doped thin films.

J. P. Chu (✉) · T. Mahalingam · C. F. Liu
Institute of Materials Engineering, National Taiwan Ocean University, Keelung 202, Taiwan
e-mail: jpchu@mail.ntou.edu.tw

S. F. Wang
Department of Materials and Minerals Resources Engineering, National Taipei University of Technology, Taipei 106, Taiwan

T. Mahalingam
Department of Physics, Alagappa University, Karaikudi 630 003, India

Introduction

Barium Titanate ($BaTiO_3$) thin films have attracted much interested in recent years due to their potential applications in various devices [1]. Due to their excellent ferroelectric and electro-optical properties, barium titanate thin films are found to be promising candidates for ferroelectric memory, electro-optic and other device applications [2, 3]. In order to improve the dielectric and ferroelectric properties, several workers have doped elements such as bismuth, lanthanum and yttrium, to tailor the defect structure [4–6]. Manganese as an acceptor-doping element influences the microstructural and electrical properties. It has been reported that Mn influences the electrical and microstructural properties of barium titanate bulk ceramics used for capacitor and positive temperature coefficient of resistivity (PTCR) devices [7, 8]. Even though several reports regarding the influence of Mn on the bulk barium titanate ceramics are available [7–10], considerably less work is carried out on the Mn-doped barium titanate in thin film form.

Several methods are employed to prepare barium titanate thin films including vacuum evaporation [11], r.f. sputtering [12], laser ablation [13], chemical vapor deposition [14] and sol–gel process [15]. When barium titanate films are deposited at low substrate temperatures by means of r.f. magnetron sputtering, they are basically amorphous [16], chemically stable and exhibit low dielectric loss as well as high optical transparency [17]. Recently, we have reported the effect of Nb doping on the structural and dielectric properties of r.f. magnetron sputtered barium titanate films [18]. The present work deals with the preparation of pure and Mn-doped barium titanate films by r.f. magnetron

sputtering. A systematic investigation of film preparation, composition analysis, crystal structure, microstructure and electrical properties is carried out. The effects of Mn doping on the microstructural and electrical properties are also presented.

Experimental procedure

Film preparation

Mn-doped barium titanate targets were prepared using commercial grade barium titanate and manganese (IV) oxide (99.999%) powder. The target discs with four Mn compositions (0.1, 0.3, 0.5 and 1.0 at%) were sintered at 1300 °C for 2 h with heating and cooling rates of 1 °C/min. X-ray diffraction studies confirmed that the prepared targets were composed of single phase. Clean glass slides, *n*-type Si (100) and Pt (250 nm thick) were used as substrates to carry out the studies for electrical measurement. The substrates were cleaned thoroughly before loading in the vacuum chamber. Pure and Mn-doped barium titanate films were prepared using a r.f. magnetron sputtering system in a high pure argon ambient as well as a mixture of argon and oxygen at a working pressure of 8×10^{-3} torr. The films were deposited without heating the substrates and the sputtering conditions are shown in Table 1. For the evaluation of electrical property measurements, Au top electrodes were deposited to form metal-insulator-metal (MIM) structure with barium titanate film as a dielectric medium. Barium titanate based thin films were rapid thermal annealed (RTA) in air at 550, 600, 650 and 700 °C for 10 s. The heating rate during the RTA process was 0.25 °C/s.

Table 1 Sputtering conditions used to prepare Mn-doped barium titanate thin films

Target composition	Pure $BaTiO_3$
	0.1%Mn-$BaTiO_3$
	0.3%Mn-$BaTiO_3$
	0.5%Mn-$BaTiO_3$
	1.0%Mn-$BaTiO_3$
Target diameter	3 inches (76.2 mm)
Target-substrate distance	80 mm
Base pressure	$<1 \times 10^{-7}$ torr
Working pressure	8×10^{-3} torr
Sputtering gas	Ar, (Ar, O_2) mixture
O_2/Ar ratio	0%, 5%, 10%, 20%, 25%, 50%
r.f. power	150 W

Characterization studies

The thickness of the barium titanate films was measured using a Tencor Alpha step profilometer and a scanning electron microscope (Hitachi S-4100). Film thickness of barium titanate thin films was estimated to be in the range between 80 and 400 nm. The composition of pure barium titanate thin films on Si wafer was analyzed by an X-ray photoelectron spectrometer (Physics Electronics, PHI 1600) with Al Kα X-rays. Structural characterization of barium titanate thin films was carried out by X-ray diffraction with a CuKα radiation. (Siemens D-5000). A Hitachi field emission electron microscope was used to analyze the planar and cross sectional views of as deposited and annealed Mn-doped barium titanate thin films. The capacitance and dielectric loss (tan δ) were measured for the Au–$BaTiO_3$–Pt MIM structures at various high frequencies (1 kHz to 1 MHz) using an impedance analyzer (HP 4194). I–V characteristics and leakage current measurements were carried out using a HP 4156C-impedance analyzer in the range from 0 to 20 kV/cm.

Results and discussion

Deposition rate and the effect of argon–oxygen atmosphere

Figure 1 shows the variation of film thickness and deposition rate with deposition time for 0.5% Mn-doped barium titanate thin films deposited on glass substrates. It is observed that the film thickness increases linearly with deposition time and the deposition rate for various sputtering times varies slightly

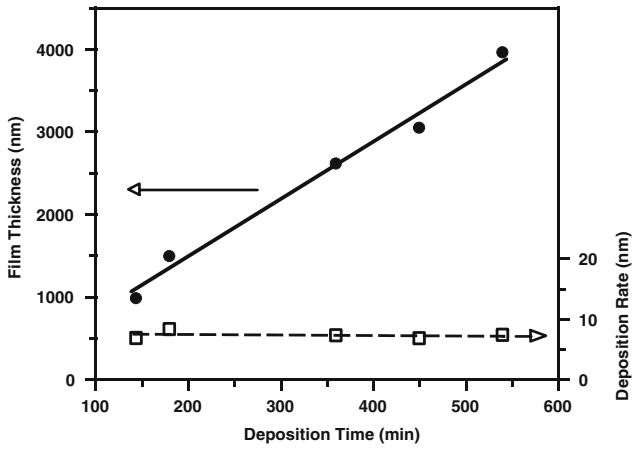

Fig. 1 Variations of film thickness and deposition rate with deposition time for 0.5% Mn-doped barium titanate thin films

from 6.8 to 8.3 with an average value of 7.3 nm/min. Argon–oxygen mixture was used as the sputtering medium to minimize the oxygen vacancy in the films resulting from the oxygen deficiency environment in the glow discharge [19]. Figure 2 shows the deposition rates of various O_2/Ar ratios for 0.5% Mn-doped $BaTiO_3$ films on glass substrates deposited for a period of 144 min. It is observed that the deposition rate increases slowly with the amount of oxygen introduced and dramatically reduced when O_2/Ar was higher than 25%. This behavior may be attributed to the formation of compound on the target and the reduction of ion energy due to excess oxygen in the sputtering atmosphere. Similar observation has been reported on the reactive sputtering of TiN in Ar and N_2 gases using a Ti target [20].

Compositional analysis

Figure 3 shows XPS spectra of a pure barium titanate film deposited on Si wafer before and after sputter etching with Ar^+ for 10 min in the binding energy range 0–1200 eV. The shift due to electrostatic charging of the sample was calibrated using the binding energy of C1s (284.6 eV). The peaks corresponding to individual elements are found in Fig. 3a. It is observed that the barium titanate film contains no impurity elements other than carbon in the entire binding energy range. The XPS survey of the specimen (curve b) after 10 min of Ar^+ sputtering is found to be free from contamination and there is no peak at 284.6 eV. This result suggests that the presence of carbon on the surface of the films is due to the contamination from the ambient. Using XPS quantitative analysis, the atomic percentages of Ba, Ti and O are estimated to be 21.7, 18.5 and 59.8, respectively.

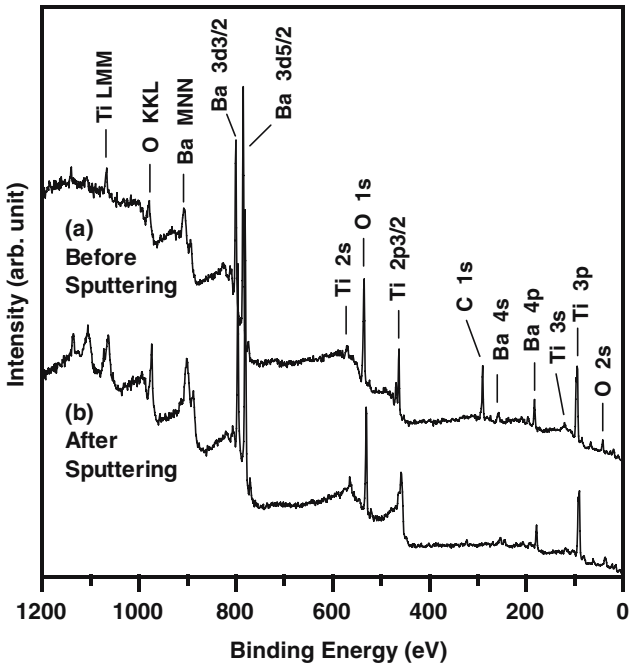

Fig. 3 XPS survey for pure barium titanate thin films on Si wafer (**a**) before and (**b**) after sputtering with Ar^+ for 10 min

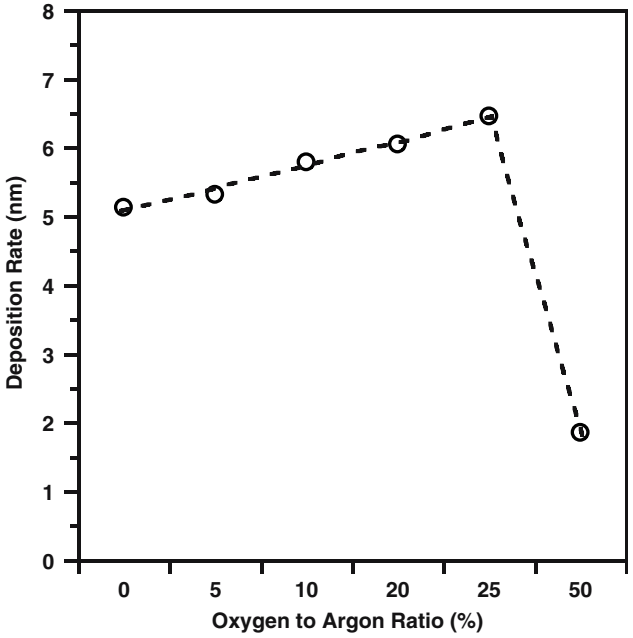

Fig. 2 Deposition rates versus O_2/Ar ratio for 0.5% Mn-doped

Structural studies

X-ray diffraction studies were carried out on as-deposited and annealed Mn-doped barium titanate thin films coated on glass substrates. It has been found that as-deposited Mn-doped barium titanate thin films at various doping concentrations are amorphous. There is no apparent variation in XRD results for as-deposited films with various Mn contents. It is observed from XRD studies that Mn-doped barium titanate thin films after annealing at 600, 630, 650 and 700 °C started to crystallize at various temperatures with the appearance of (110) peak. However, pure barium titanate thin films were still found to possess amorphous nature with annealing temperatures between 600 and 650 °C. X-ray diffraction patterns of a representative 0.5% Mn-doped barium titanate thin film annealed at various temperatures are shown in Fig. 4. It is observed that the film starts to crystallize with the appearance of (110) peak at 630 °C and became fully crystalline when annealed at 700 °C.

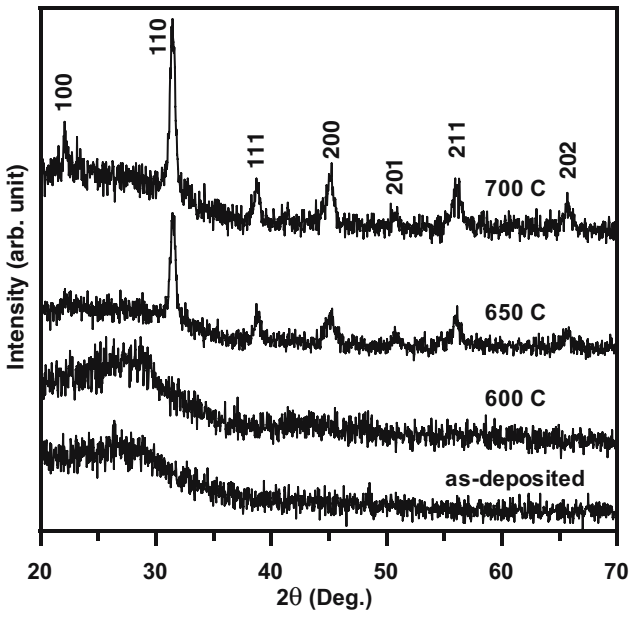

Fig. 4 XRD patterns of 0.5% Mn-doped barium titanate thin films annealed at various temperatures

Figure 5 exhibits the XRD patterns of various Mn-doped barium titanate thin films along with the pure barium titanate film annealed at 700 °C. It is observed that the pure barium titanate and doped barium titanate thin films are well crystallized after annealing at 700 °C. Our XRD studies indicate that the crystallization of the film takes place between 600 and 650 °C depending on the Mn content. The addition of Mn assists the film crystallization and lowers the crystallization temperature.

The lattice parameters (c and a) of the targets and films are estimated and the structure of $BaTiO_3$ targets is found to be primarily tetragonal with a c/a ratio of 1.01 for pure $BaTiO_3$. The tetragonality of pure $BaTiO_3$ film annealed at 700 °C is found to be 1.003. The tetragonality values are found to be 1.002, 1.005, 1.000 and 1.006 for $BaTiO_3$ films doped with 0.1, 0.3, 0.5 and 1.0 % Mn, respectively. Since the tetragonality factor is close to 1, it appears that Mn-doped barium titanate thin films prepared by r.f. magnetron sputtering exhibits primarily cubic structure. Wang et al. [21] reported a perovskite cubic structure for their r.f. magnetron sputtered barium titanate films. The lattice parameter is calculated based on the XRD patterns and its variation with Mn doping is shown in Fig. 6. It is observed that the lattice parameter decreases from 0.4041 nm for pure barium titanate film to 0.3995 nm for 1.0% Mn-doped barium titanate film. Since very small quantities of Mn are doped with $BaTiO_3$ film, the XRD pattern does not reveal any peak corresponding to the presence of Mn. Another possible reason for the absence of any peak in the XRD pattern is that the Mn^{2+} ions with radius 0.067 nm might have completely incorporated into $BaTiO_3$ lattice through Ti^{4+} sites (radius 0.068 nm). The full width at half maximum (FWHM) of annealed Mn-doped samples (Fig. 5) for (110) Bragg peak is found to be relatively broad indicating the smaller grain sizes for annealed films. It has been reported that when the grain size decreases sufficiently, the unit cell becomes less tetragonal resulting in a pseudo cubic phase [22, 23].

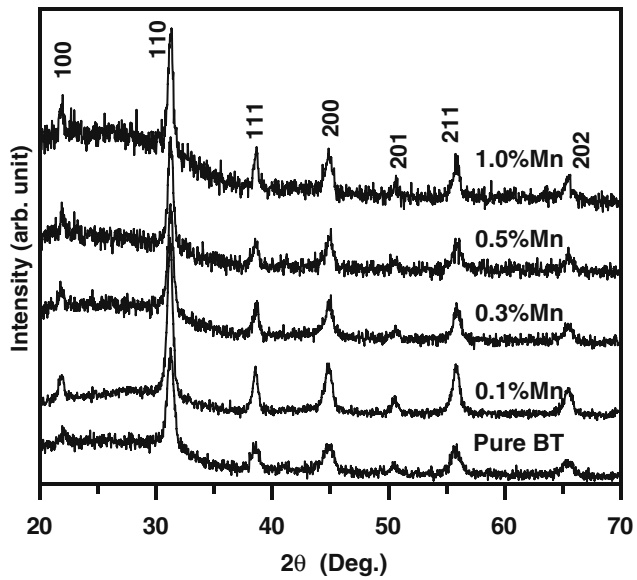

Fig. 5 XRD patterns of various Mn-doped barium titanate thin films annealed at 700 °C

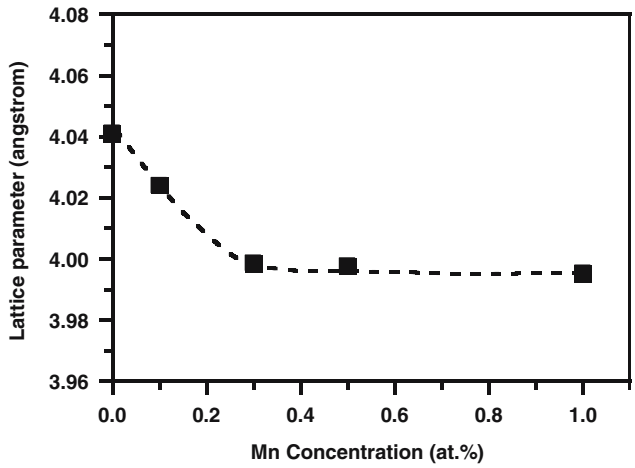

Fig. 6 Variation of lattice parameter with Mn doping in barium titanate thin films

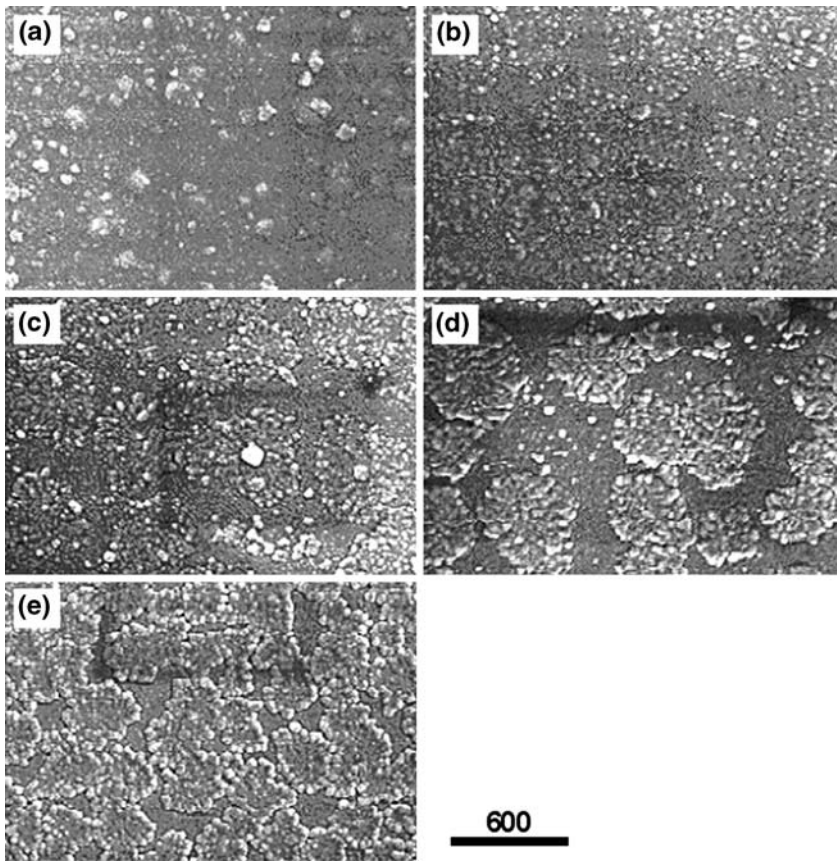

Fig. 7 Plane view SEM micrographs of Mn-doped films annealed at 650 °C. Mn concentrations: (**a**) 0%, (**b**) 0.1%, (**c**) 0.3% (**d**) 0.5% and (**e**) 1.0%. Scale bar: 600 nm

Microstructure

The surface morphology of $BaTiO_3$ films was analyzed using a scanning electron microscope. Figure 7 shows the plane view scanning electron micrographs of various Mn-doped $BaTiO_3$ film annealed at 650 °C in the RTA furnace for 10 s. The plane view surface morphology reveals the presence of granular structures and clusters characteristics of high temperature annealed films. The clusters are found to become large and dense with the increase of Mn contents. Hemispherical shaped island like grains are also seen and similar morphology is commonly observed in ceramic thin films such as $BaSrTiO_3$ and $PbZrO_3$ prepared by physical vapor deposition. The surface morphology of $BaTiO_3$ films also reveals a fine grain microstructure without any cracks. Similar surface morphology is observed in sol–gel prepared Sr doped [24], and r.f sputtered Ce doped [25] $BaTiO_3$ thin films.

Electrical property measurement

The dielectric properties of the Mn-doped $BaTiO_3$ thin films (Au–$BaTiO_3$–Pt) were measured in the frequency range between 1 kHz and 1 MHz. The variation of dielectric constant and tan δ of $BaTiO_3$ based thin films measured at 1 MHz and at 25 °C is shown in Fig. 8. It is observed that the dielectric constant increases with Mn doping. However, the dielectric loss (tan δ), shows a minimum value of 0.0054 for 0.5% Mn-doped $BaTiO_3$ film which indicates that the 0.5% Mn doping as the optimum doping level to prepare films for capacitor applications. Sasaki et al. [26] observed that the dielectric constants of ion beam sputtered Sb

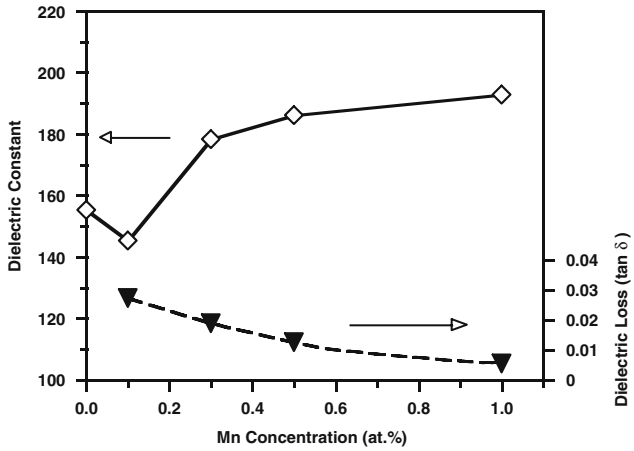

Fig. 8 Variation of dielectric constant and tanδ at 1 MHz with Mn doping in barium titanate thin films

doped $BaTiO_3$ films were in the range of 80–100 and further reported that there was no marked variation of dielectric constant with antimony doping. The low values of dielectric constant observed in the present study may be attributed to the small grain sizes of the films as observed by SEM and the broadening of the XRD peaks of annealed Mn-doped $BaTiO_3$ films. Similar microstructural and dielectric properties have been reported for $BaTiO_3$ thin films earlier [27]. The possible existence of a non-ferroelectric surface layer at the film-electrode interface may also be responsible for the reduction of dielectric constant in the films [28].

The current–voltage characteristics of MIM structure employing annealed Mn-doped $BaTiO_3$ films are carried out. It is observed that at low electric fields (<6 kV/cm) an exponential increase of current with electric field is observed followed by saturation at high electric fields. It is observed that the leakage current is around 10^{-8} A/cm^2 for 0.1% Mn-doped $BaTiO_3$ film and it decreases to 10^{-11} A/cm^2 for 1.0% Mn-doped $BaTiO_3$ film.

Conclusions

Mn-doped $BaTiO_3$ thin films have been deposited by r.f. sputtering at various O_2/Ar gas mixing ratios at room temperature. As-deposited $BaTiO_3$ films are found to be amorphous and annealed films at 700 °C yields cubic films with perovskite structure. It is found that the lattice parameter of Mn-doped annealed $BaTiO_3$ films decrease with increase in Mn content. O_2/Ar gas ratio is found to exhibit maximum sputtering rate in r.f. sputtered films. The dielectric constant is found to increase with Mn content and the dielectric loss (tan δ) reveals a minimum value for 0.5% Mn-doped $BaTiO_3$ films. The leakage current density decreases with Mn doping and found to be very small (10^{-11} A/cm^{-2}) for 1% Mn-doped $BaTiO_3$ thin films.

Acknowledgements This work is supported by National Science Council of Republic of China (NSC-92-2216-E-027-007 and NSC-92-2216-E-019-004), which is gratefully appreciated.

References

1. Preda L, Couselle L, Despax B, Bandet J, Ianculescu I (2001) Thin Solid Films 389:43
2. Dimos D (1995) Ann Rev Mater Sci 25:273
3. Lu HA, Wills LA , Wessels WB (1994) Appl Phys Lett 64:2973
4. Kubo R, Xu H, Yoshino Y, Okuyama N (1998) Mater Res Soc Symp Proc 526:181
5. Ardakani HK, Shushtarain SS, Kanetkar SM, Karekar RN, Ogale SB (1993) J Mater Sci Lett 12(9):63
6. Choi WY, Tsur T, Randall CA, Trolier-McKinstry S (2009) Mater Res Soc Symp Proc 596:487
7. Hagemann H-J, Ihrig H (1979) Phys Rev B 20:3871
8. Desu SB, Subbarao EC (1981) Ferroelectrics 37:665
9. Burn J (1979) J Mater Sci 14:3871
10. Langhammer HT, Muller T, Felgner K-H, Abicht H-P (2000) Mater Lett 42:21
11. Kwak BS, Zhang K, Boyd EP, Erbil A, Wilkens BJ (1991) J Appl Phys 69:767
12. Fujimoto K, Kobayashi Y, Kubota K (1989) Thin Solid Films 169:249
13. Roy D, Krupanidhi SB (1992) Appl Phys Lett 61:2057
14. Nakazawa H, Yamane H, Hirai T (1991) Jpn J Appl Phys 30:2200
15. Kamalasanan MN, Kumar ND, Chandra S (1994) J Appl Phys 76:4603
16. Chu JP, Wang SF, Lee SJ, Chang CW (2000) J Appl Phy 88:6086
17. Pencheva T, Nenkov M (1997) Vacuum 48:43
18. Chu JP, Chang CW, Mahalingam T, Lin CC, Wang SF (2003) J Mater Sci Lett 22:1269
19. Salama CAT , Siciunas E (1972) J Vac Sci Technol 9:91
20. Kawamura M, Abe Y, Yanagisawa H, Sasaki K (1996) Thin Solid Films 287:115
21. Wang MC, Hsiao FY, His CS, Wu WC (2002) J Cryst Growth 246:78
22. Takeuchi T, Tabuchi M, Kageyama H (1999) J Am Ceram Soc 82:939
23. Caboche G, Chaput F, Boilot JB, Niepce JC (1993) Silicates Indutries 5–6:103
24. Tian HY, Luo NG, Pu XH, Ding AL (2000) J Mater Sci Lett 19:1211
25. Cernea M, Matei I, Iuga A, Logofatu C (2001) J Mater Sci 36:5027
26. Sasaki Y, Fuji I, Matsui T, Morii K (1996) Mater Lett 26:265
27. Lee B, Zhang J (2001) Thin Solid Films 388:107
28. Kawano T, Sei T, Tsuchida T (1991) J Mater Sci 31:2178